



# Comparison of corncob-derived solid acids and evaluation of catalytic cellulose hydrolysis performance in LiBr

Chen Liang<sup>1</sup> · Chunhua Du<sup>1</sup> · Xianli Wu<sup>1</sup> · Ju Wang<sup>1</sup> · Jie Xu<sup>1</sup> · Pengyu Hu<sup>2</sup> · Wangda Qu<sup>2</sup>

Received: 16 November 2021 / Revised: 31 December 2021 / Accepted: 6 January 2022 / Published online: 13 January 2022  
© The Author(s), under exclusive licence to Springer-Verlag GmbH Germany, part of Springer Nature 2022

## Abstract

In order to enhance the valorization of corncob, corncob-based solid acid catalysts were prepared via the method of partial carbonization followed by sulfonation. The prepared acid catalysts were either derived from raw corncob (hemicellulose, cellulose, and lignin), or its residues after different pretreatments, i.e., furfural residue (cellulose and lignin) and hydrolysis residue (humins and lignin), to investigate the components' effect on the performance of solid acid. These catalysts were characterized by thermogravimetric analysis (TGA), Fourier transform infrared spectroscopy (FTIR), X-ray diffraction (XRD), nitrogen adsorption/desorption analysis, scanning electron microscope (SEM), elemental analysis, and acid–base titration. The analysis results suggested that the solid acid (Catalyst-3) derived from the hydrolysis residue had the best performance, with a BET surface area of 338.23 m<sup>2</sup> g<sup>-1</sup> and total acid densities of 6.43 mmol g<sup>-1</sup>. This results indicated –SO<sub>3</sub>H groups were loaded onto the catalyst successfully. The catalytic activity was tested by cellulose hydrolysis in lithium bromide trihydrate solution (LBTH) system. The yield of glucose was as high as 80.1% at the temperature of 110 °C for 10 h. Moreover, the prepared solid acid had the advantages of easy separation, mild reaction, and producing less by-products compared with traditional liquid acids. This work provides a promising strategy for corncob waste utilization and cellulose efficient hydrolysis, which is of great significance for biomass valorization and conversion.

**Keywords** Cellulose hydrolysis · Carbon-based solid acid · Corncob · LiBr molten salt · Catalysis

## 1 Introduction

The depletion of fossil fuels has caused issues in energy security globally, so there is sparking interest in finding alternative renewable energy sources [1]. As the most abundant renewable resource, biomass has the advantages of wide distribution and availability, along with its environment-friendliness. As a result, conversion of biomass to chemicals has attracted tremendous research interests, and biomass-derived fuels or materials has been widely investigated [2, 3]. Particularly, in the field of lignocellulosic biomass conversion, it is widely accepted that efficient conversion of cellulose to glucose is crucial for the production

of fuel or chemicals from biomass [4]. Cellulose is a linear polymer, and it is composed of repeatable basic units of β-(1–4) glycosidic linkages. There are extensive hydrogen bonds due to the existence of intra- and inter-chain of cellulose, resulting in the extreme stability of cellulose. In order to fulfill the effective decomposition of cellulose to glucose, it is necessary to adopt reasonable ways to address the issues in cellulose conversion [5].

To date, enzymatic and acid hydrolyses of cellulose are the most conventional treatment methods. Enzymatic hydrolysis has been regarded as a mild treatment for cellulose conversion, but it has the disadvantages of long production cycle and poor recyclability [6, 7]. Acid hydrolysis has a relatively higher efficiency, and various acid catalysts including homogeneous and heterogeneous catalysts have been studied in cellulose saccharification process. In homogeneous catalysts, H<sub>2</sub>SO<sub>4</sub> and HCl are the most common catalysts. Although they have high activities, their commercial applications are hard to accomplish owing to the issues of corrosion, poor selectivity, and difficulties in waste treatment [8, 9]. To overcome the defect of mineral acids, the heterogeneous catalysts

✉ Wangda Qu  
wqu@qau.edu.cn

<sup>1</sup> College of Chemistry and Pharmacy, Qingdao Agricultural University, 700 Changcheng Road, Qingdao, People's Republic of China

<sup>2</sup> College of Life Sciences, Qingdao Agricultural University, 700 Changcheng Road, Qingdao, People's Republic of China

such as H-zeolites [10], transition-metal oxides [11], cation-exchange resins [12], heteropoly acid [13], urea nitrate [14], and carbon-based solid acid [15–18] have been proposed and investigated. Among the various solid acids, carbon-based solid acid has the advantage of higher activity and thermal stability, and good recyclability [19]. Particularly, carbon-based solid acids have recently caught much attention in the field of cellulose conversion. Carbon-based solid acids can be made from wide biomass species such as rice husk [20], bamboo [21], sugar cane [22], palm kernel shell [23], and corncobs [24]. Among the biomasses mentioned above, corncob is a type of biomass with important commercial value. In the biorefining process of corncob, the utilization of hemicellulose and cellulose from corncobs has been commercialized via its derived products, i.e., xylose, furfural, bioethanol, and other chemicals [25–27]. However, after conversion, the hemicellulose and cellulose, the remaining components remained underutilized. Moreover, in the field of carbon-based solid acid, previous studies mostly investigate the performance of a certain carbon-based solid acid, but did not specifically study the effect of solid acid deriving from different components in the same biomass. In the context of the demand of the corncob industry and research insights of solid acid, it is necessary to investigate the influence of different corncob components on the performance of catalyst, upon converting corncob residue into different types of solid acids.

In addition to the catalysts, the catalytic solution system also plays an important role in determining hydrolysis efficiency. Aqueous system is the most popular catalytic solution system. Inorganic acid catalysts such as  $H_2SO_4$  and HCl have high catalytic efficiency in aqueous phase system but there are many problems. On the other hand, for solid acid catalysts, approaching the  $\beta$ -(1–4) glycosidic linkages in aqueous system is difficult for the active sites, resulting in low hydrolysis efficiency [28]. Relatively high temperature or ball milling pretreatment of cellulose can improve the hydrolysis efficiency to some extent [29, 30]. However, the costs of the above methods are high. Another promising solution system is ionic liquids [31]. In some ionic liquids, cellulose could be dissolved for the hydrogen bonds between cellulose and anions in ionic liquid [32]. Therefore, the active sites can better cut off the  $\beta$ -(1–4) glycosidic linkages. The 1-butyl-3-methylimidazolium chloride ([BMIM] Cl) was chosen as the most popular solution in cellulose dissolution [33]. However, the synthesis of ionic liquids is complex and expensive [34, 35]. Additionally, for heterogeneous catalysts, the hydrolysis efficiency in pure ionic liquids is not ideal unless water is supplemented [15]. The recyclability of ionic liquid also limits its large-scale application [36]. In recent years, lithium bromide trihydrate solution system is considered to have a good dissolution ability of cellulose. In LBTH system, cellulose can be hydrolyzed at relatively

low acid concentration and low temperature [37, 38]. Deng et al. found that cellulose could be effectively hydrolyzed to glucose at 85 °C and low acid concentration in LiBr system [39]. Wu et al. adopted zeolite as catalyst to convert cellulose into glucose in LiBr system at 140 °C, and high glucose yield of 61% was achieved [10]. The oligomers from cellulose hydrolysis has high solubility in molten salt hydrates and can be further separated by adsorption [40]. Therefore, hydrolysis of cellulose in LiBr molten salt hydrates is a promising method.

In general, hydrolysis of lignocellulose into reducing sugar is the key step for biorefinery of biomass. Both solution system and catalyst play significant roles in cellulose hydrolysis. In this study, solid acid catalysts prepared from corncob at different pretreatment stages were used for catalytically hydrolyzed cellulose in the LBTH system. The correspondingly derived carbon-based solid acids were evaluated for their activities. The performance of catalytic cellulose hydrolysis in LiBr molten salt was further carried out. The plausible mechanism for the cellulose hydrolysis in LBTH system over the prepared solid acids was proposed. Compared with the previous cellulose saccharification technology, the process reported here has the superiority of applying mild conditions, producing less by-products and high glucose yield. This study provides a novel strategy in the field of cellulose efficient hydrolysis and corncob valorization.

## 2 Materials and methods

### 2.1 Materials

The experimental materials used in this work were presented as follows: 50-mesh corncobs (Shengqiang farm, China), 96 wt% sulfuric acid (Sinopharm Chemical, China), glucose (Sinopharm Chemical, China), microcrystalline cellulose (Macklin, China), levulinic acid (Aladdin, China), and lithium bromide (Aladdin, China).

### 2.2 Experimental procedure

#### 2.2.1 Pretreatment of corncob

Corncobs were dried by a vacuum oven (TD-500, Guansen Biology, China) at 105 °C and recorded as Material-1 (main composition: hemicellulose, cellulose, and lignin).

The corncobs were mixed with 3 wt% sulfuric acid and reacted at 100 °C with solid-to-liquid ratio of 1:10 for 3 h to effectively remove the hemicellulose from corncobs [41]. Then, the corncob residues were filtered and washed. Finally, the corncob residue was dried and marked as Material-2 (main composition: cellulose and lignin).

The Material-2 were added into a autoclave reactor with sufficient 5 wt% sulfuric acid, and maintained at 180 °C for 3 h to decompose cellulose [42]. After hydrolysis and drying, the hydrolysis residue was named as Material-3 (main composition: lignin and humins).

### 2.2.2 Catalyst preparation

The Material-1 was loaded in a crucible and placed in the GSL-1700X tube furnace (Kejing Instruments, China). The heating rate of the tubular furnace was set at 5 °C min<sup>-1</sup> to 400 °C and maintained for 2 h. During carbonization in tubular furnace, purified N<sub>2</sub> was introduced into the reactor as protective gas. The carbonized Material-1 was named Carbon-1. About 5 g of carbon was mixed with 50 mL of 96 wt% sulfuric acid and reacted at 120 °C for 10 h. Then, the catalyst was thoroughly washed with deionized water until neutral pH. Finally, the prepared solid acid was dried and recorded as Catalyst-1.

Material-2 and Material-3 adopted the same conditions as Material-1 to prepare the carbons and catalysts. The carbonized samples from Material-1, Material-2, and Material-3 were designated as Carbon-1, Carbon-2, and Carbon-3, respectively.

### 2.2.3 Cellulose hydrolysis with solid acid

**Cellulose hydrolysis** The cellulose hydrolysis was carried out at the temperature of 90 °C, 100 °C, and 110 °C, respectively. In the reaction, 1-g cellulose and 60-mL LiBr solution (55 wt%) were first added to a 100-mL three-necked flask reactor and heated to the target temperature in the oil bath to form a transparent solution. When the temperature was stable, 0.5 g of solid acid was added to the system. The mixing speed was set to 500 rpm. As the reaction progressed, the sample was taken out and then filtered with a 0.45-μm filter membrane. The samples were then characterized for component concentrations by a high performance liquid chromatography system (HPLC).

**Recyclability of the catalyst** The recyclability test was carried out at 110 °C for 6 h. The reaction parameters were consistent with the above part. After the reaction, the used catalyst was filtered, washed, and dried in an oven for 8 h. The filtrate was sent to HPLC to detect the hydrolysis efficiency. The process was repeated several times to evaluate the recyclability of the catalyst.

### 2.3 Catalyst characterization

TG and DTG were performed by a TG Q500 thermal analyzer (TG Instruments, USA). About 10 mg sample was heated at N<sub>2</sub> atmosphere from room temperature to 1000 °C. FTIR was conducted by a Thermo Scientific Nicolet iS10 (Thermo Fisher

Scientific, Inc., USA), and the detection wavelength was set as 750–4000 cm<sup>-1</sup>. The catalyst structure was determined by the XRD instrument of D8 Advance (Bruker, Germany), with the scanning range of 2θ from 5° to 60°. The total surface area, distribution of pore size and pore volume were estimated by N<sub>2</sub> adsorption–desorption analysis conducted by Sorptomatic 1990 series (Thermo Finnigan, USA). The microstructures of the catalyst were examined with a JEOL-7500F scanning electron microscope (Hitachi, Japan). Elemental compositions of the catalyst samples were detected by an elemental analyzer of Vario EL cube (Elementar, Germany).

Acid–base titration method was adopted to measure the total acid density of the catalyst. The 30 mL of 50-mmol L<sup>-1</sup> NaOH solution was mixed with 0.1 g of catalyst and stirred for 120 min. After the reaction, 20 mL of the solution with the phenolphthalein indicator was titrated to neutral pH by the 50-mmol L<sup>-1</sup> standard acid. The consumed standard acid volume was recorded as V mL. It is assumed that NaOH can neutralize all acidic groups (–OH, –COOH, and –SO<sub>3</sub>H) in catalyst. The neutralized NaOH can be further calculated according to the consumption of acid standard solution, using the following equation:

$$\text{Total acid density} = 1.5 \times \left( \frac{20}{1000} \times 50 - \frac{V}{1000} \times 50 \right) \times 10 \quad (1)$$

### 2.4 Analysis

The glucose and levulinic acid (LA) contents were analyzed by HPLC of L-2000 (Hitachi, Japan). The chromatographic column was selected as HPX-87H with the size of 300 mm × 7.8 mm (Bio-Rad, USA). The mobile phase was 5-mmol L<sup>-1</sup> sulfuric acid, and the flow rate was set as 0.55 mL min<sup>-1</sup>. The column temperature was set to 60 °C, and the detector temperature was set to 38 °C. The yield of glucose and LA were calculated using equations:

$$\text{Glucose yield} = \frac{\text{molar concentration of glucose}}{\text{molar concentration of cellulose}} \quad (2)$$

$$\text{LA yield} = \frac{\text{molar concentration of LA}}{\text{molar concentration of cellulose}} \quad (3)$$

## 3 Results and discussions

### 3.1 Catalyst characterizations

#### 3.1.1 TG and DTG

Firstly, the thermal stability of the catalysts prepared from three corncob-derived materials was analyzed, and the TG

curve is shown in Fig. 1. It can be seen from the TG diagram that as the temperature increases, the weight loss of the three catalysts (as described in the experimental method, Catalyst-1 was prepared from untreated corncob; Catalyst-2 uses xylose residue as raw material; Catalyst-3 comes from hydrolysis residue), and the pyrolysis yields were almost identical, indicating that they had similar thermal stability. It illustrated that although the raw materials of the three catalysts were different, different components in the materials would form a relatively stable structure after incomplete carbonization and sulfonation.

In order to discuss the differences of the catalysts, the DTG results of catalysts are studied, as shown in Fig. 2. The catalysts had a weight loss peak at around 300 °C. The reason for the weightlessness interval may be that the  $-\text{SO}_3\text{H}$  group supported on the catalyst was unstable and easily decomposes at this temperature. To verify the hypothesis, the DTG of Carbon-1, Carbon-2, and Carbon-3 were further investigated, and the analysis results are presented in Fig. 3.

It can be seen from Fig. 3 that at around 300 °C, three carbons had no obvious weight loss peak. The reason was that the Carbon-1, Carbon-2, and Carbon-3 had already been carbonized. The pyrolysis of the materials before 400 °C has been completed at carbonization stage. The comparison in Figs. 2 and 3 fully proved that the weight loss peak at about 300 °C is the pyrolysis of  $-\text{SO}_3\text{H}$  group. In addition, it also could be found in Fig. 2 that the weight loss of Catalyst-1 is the most, Catalyst-2 is the second, and Catalyst-3 is the least, proving that the  $-\text{SO}_3\text{H}$  groups supported by the Catalyst-3 had the highest concentration.

### 3.1.2 XRD analysis

The crystalline structure of the three catalyst samples was analyzed, and the data are presented in Fig. 4. As can be seen

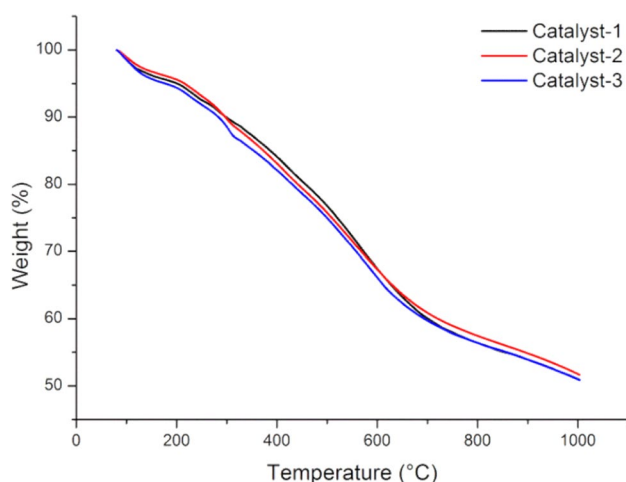


Fig. 1 TG of Catalyst-1, Catalyst-2, and Catalyst-3

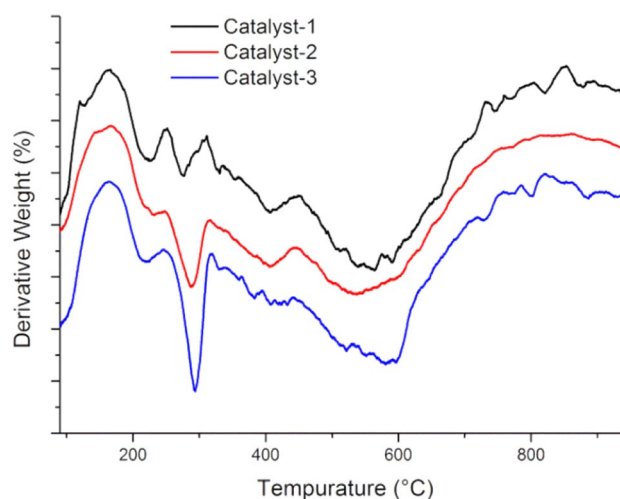


Fig. 2 DTG of Catalyst-1, Catalyst-2, and Catalyst-3

from the profile, a broad diffraction peak appeared at  $2\theta$  of around  $25^\circ$ . This was considered to be the amorphous carbon structure formed by polycyclic aromatic compounds. The structure of amorphous carbon was easy to introduce  $-\text{SO}_3\text{H}$  group on catalyst [43]. It can be observed that there was no noticeable difference in the crystalline structure for these three samples, indicating that the differences in raw material components did not influence the crystalline structure of the catalyst.

### 3.1.3 FTIR analysis

FTIR analysis was conducted to understand the differences of the carbon and catalysts. In the spectra of three carbons

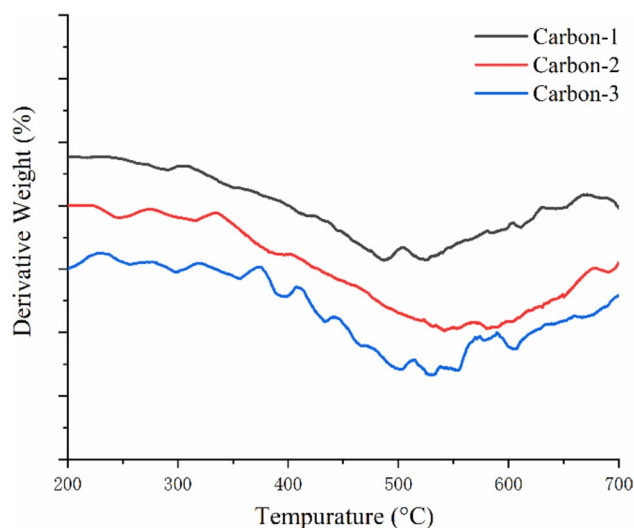
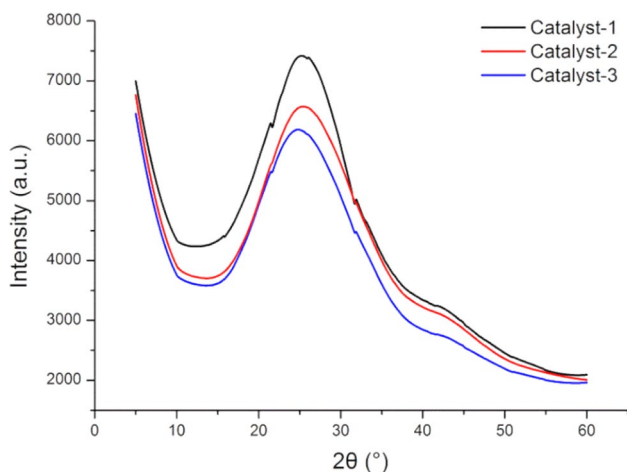
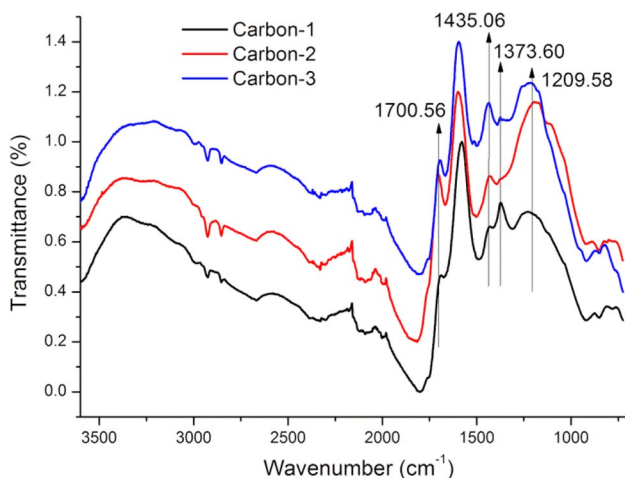


Fig. 3 DTG of Carbon-1, Carbon-2, and Carbon-3



**Fig. 4** XRD spectrum of Catalyst-1, Catalyst-2, and Catalyst-3

(Fig. 5), there was a peak at around  $1209\text{ cm}^{-1}$ . This pattern of Carbon-2 was the most, Carbon-3 was the second, and Carbon-1 was the least. The band at around  $1209\text{ cm}^{-1}$  was ascribed to C–C, C–O or C=O stretching, demonstrating Carbon-2 contained more such structures. The Carbon-3 had an obvious peak at around  $1373\text{ cm}^{-1}$ , while there was almost no peak in Carbon-2 and Carbon-1. The band at around  $1373\text{ cm}^{-1}$  was considered as the aliphatic C–H stretch in  $\text{CH}_3$ , indicating that Carbon-1 contains aliphatic hydrocarbons. The band at around  $1435\text{ cm}^{-1}$  was regarded as the aromatic skeletal vibrations combined with C–H in-plane deform. The peak of Carbon-3 in  $1435\text{ cm}^{-1}$  was the most. The reason may be that Carbon-3 was prepared from Material-3 (main components: lignin and humins), which had a more aromatic structure, leading to the noticeable peak. In addition, the band at around  $1700\text{ cm}^{-1}$  was observed in all the spectra, which attributed to the C=O in



**Fig. 5** FTIR spectra of Carbon-1, Carbon-2, and Carbon-3

–COOH groups. There were some differences in the FTIR spectra of the three catalysts, and these differences were attributed to different components of materials.

In the FTIR spectrum of Catalyst-3 in Fig. 6, the bands at around  $1031\text{ cm}^{-1}$  are ascribed to S=O stretching modes of  $-\text{SO}_3\text{H}$ , indicating the successful introduction of  $-\text{SO}_3\text{H}$  to the carbon material. At the peak of  $1700\text{ cm}^{-1}$ , the bond in Catalyst-3 was more obvious than Carbon-3, indicating that more –COOH was introduced into the catalyst in the sulfonation process. In the spectrum of Carbon-3, there was a peak at  $1435\text{ cm}^{-1}$ , but it was not obvious in Catalyst-3, demonstrating that the C–H bond was replaced by C– $\text{SO}_3\text{H}$  in the sulfonation process. Therefore, the overall results demonstrated the existence of  $-\text{SO}_3\text{H}$ , –COOH groups in the carbon-based solid acid. It was considered that a catalyst loaded with –OH, –COOH, and  $-\text{SO}_3\text{H}$  groups had a stronger attraction to  $\beta$ -(1–4) glycosidic linkages in cellulose than the catalyst with only  $-\text{SO}_3\text{H}$  added [43].

The FTIR spectra of the Catalyst-1, Catalyst-2, and Catalyst-3 are further compared in Fig. 7. Interestingly, the results showed that FTIR of the three catalysts was quite similar. However, it can be seen from Fig. 5 that the difference of the three carbons is obvious before sulfonation. It was speculated that the sulfonation process was a remodeling process. In addition to the introduction of the  $-\text{SO}_3\text{H}$  groups, other groups on the catalyst surface will also be further rearranged and cyclized. The slight differences in Fig. 7 are further analyzed. For example, the peak at  $1031\text{ cm}^{-1}$  of Catalyst-1 was significantly weaker than that of Catalyst-2 and Catalyst-3, indicating that  $-\text{SO}_3\text{H}$  groups supported by Catalyst-1 was relatively small. However, it was difficult to distinguish the differences at the bond of  $1031\text{ cm}^{-1}$  for Catalyst-2 and Catalyst-3, therefore their abundance of  $-\text{SO}_3\text{H}$  groups needs further verification.

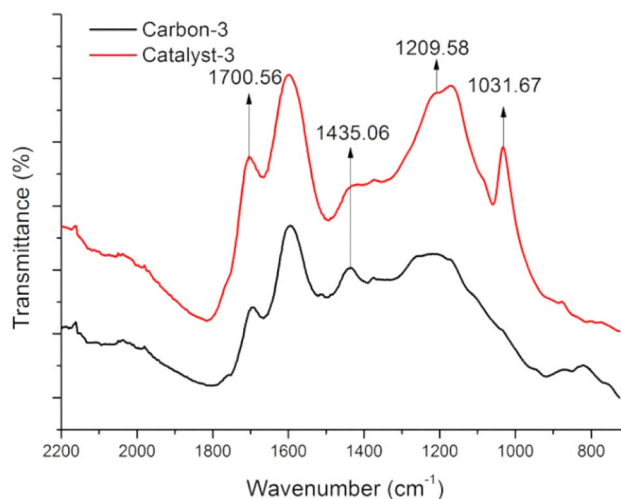


**Fig. 6** FTIR spectra of Carbon-3 and Catalyst-3



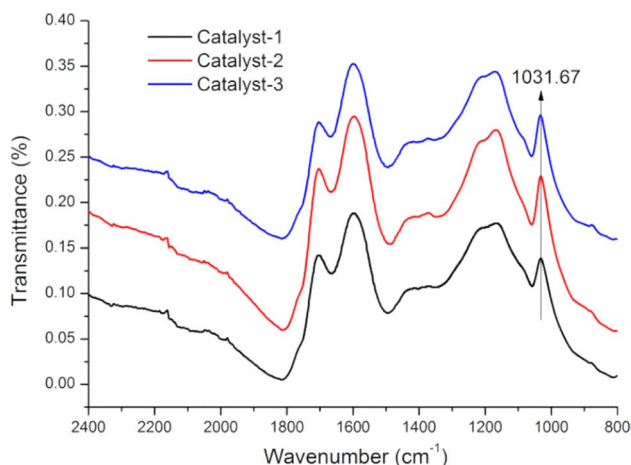


**Fig. 7** FT-IR spectra of Catalyst-1, Catalyst-2, and Catalyst-3

### 3.1.4 Elemental analysis

To investigate the sulfonation effect of solid acid, elemental analysis of the samples was conducted, and the results were presented in Table 1. From the elemental analysis of Carbon-1, Carbon-2, and Carbon-3, the carbon content of Carbon-1 was the lowest, followed by Carbon-2, and the Carbon-3 was the highest, while the oxygen content was increased inversely opposing to carbon content trend. This demonstrated that the carbon content in the corncobs gradually increases after removing hemicellulose and cellulose separately. This conclusion was consistent with the carbon yield obtained from the experimental results: after carbonization, the carbon yield of Material-1, Material-2, and Material-3 were 35%, 40%, 58%, respectively. Before sulfonation, the content of sulfur in the three carbon products was very low. After sulfonation with concentrated sulfuric acid, the oxygen and sulfur contents of the sample increased significantly, indicating that the three carbons were successfully loaded with  $-\text{SO}_3\text{H}$  groups. Through comparison, it can be seen that the sulfur element in Catalyst-3 was larger than that in Catalyst-1 and Catalyst-2 and it proved that more  $-\text{SO}_3\text{H}$  groups were loaded on Catalyst-3. The results of the elemental analysis were in accordance with FTIR results.

**Table 1** Element content of catalyst and carbon

Sample	N + P [%]	C [%]	H [%]	S [%]	O [%]
Carbon-1	0.69	62.84	2.297	0.038	34.25
Carbon-2	0.56	64.95	2.727	0.058	31.55
Carbon-3	0.53	67.31	2.947	0.055	29.15
Catalyst-1	0.68	46.32	2.619	2.321	48.06
Catalyst-2	0.46	47.46	2.802	2.658	46.62
Catalyst-3	0.38	48.87	2.967	2.713	45.07

### 3.1.5 $\text{N}_2$ adsorption/desorption analysis

The  $\text{N}_2$  adsorption/desorption analysis was conducted to measure the BET surface area of catalysts, and the data were summarized in Table 2.

According to the results, macropores were mainly present in Catalyst-1 and Catalyst-2. Upon removal of hemicellulose, the total surface area was slightly increased but still as low as  $15.01 \text{ m}^2 \text{ g}^{-1}$ . Interestingly, the BET surface area of the Catalyst-3 was significantly higher than that of Catalyst-1 and Catalyst-2, reaching to  $338.23 \text{ m}^2 \text{ g}^{-1}$ . Through data analysis, it can be concluded that a large number of micropores were generated in Catalyst-3, proving that many micropores were formed in the process of corncob hydrolysis of cellulose. The reason may be that when hemicellulose was reacted, the original surface of the corncob was destroyed, and some macropores were formed. But when the cellulose was hydrolyzed, many pores will be formed where the cellulose was originally filled. The remaining lignin microspheres will further agglomerate and the microporous structures will be formed during the agglomeration of microspheres, resulting in a significant increase of the BET surface area. The presence of micropores usually increased the contact between the reactants and catalyst, thereby increasing the catalytic effect.

### 3.1.6 SEM

In order to investigate the morphological characteristics of the catalyst, SEM images of samples were further studied. As shown in Fig. 8a, the morphology features of Catalyst-1 show large aggregates with flat and smooth surfaces. An obvious change of the morphology feature was observed for Catalyst-2 (Fig. 8b): the surface of the catalyst became disordered and a rougher structure was revealed, while no porous structure was formed. In Fig. 8c, the morphology of the Catalyst-3 shows more porosities, and the particle decreased in size. Figure 8d is an enlarged view of Fig. 8c, which shows that there were many microporous structures between lignin microspheres (as circled in the image). The analysis results from SEM results can further confirm the hypothesis on the formation mechanism of the catalyst micropores.

**Table 2** The  $\text{N}_2$  adsorption/desorption analysis of the catalysts

Sample	Mean pore diameter (nm)	Total pore volume ( $\text{cm}^3 \text{ g}^{-1}$ )	BET surface area ( $\text{m}^2 \text{ g}^{-1}$ )
Catalyst-1	150.56	$4.23 \times 10^{-3}$	3.98
Catalyst-2	83.68	$2.36 \times 10^{-2}$	15.01
Catalyst-3	2.35	$3.72 \times 10^{-1}$	338.23

**Fig. 8** SEM morphology of (a) Catalyst-1 with 10  $\mu\text{m}$ , (b) Catalyst-2 with 10  $\mu\text{m}$ , (c) Catalyst-3 with 10  $\mu\text{m}$ , and (d) Catalyst-3 with 1  $\mu\text{m}$

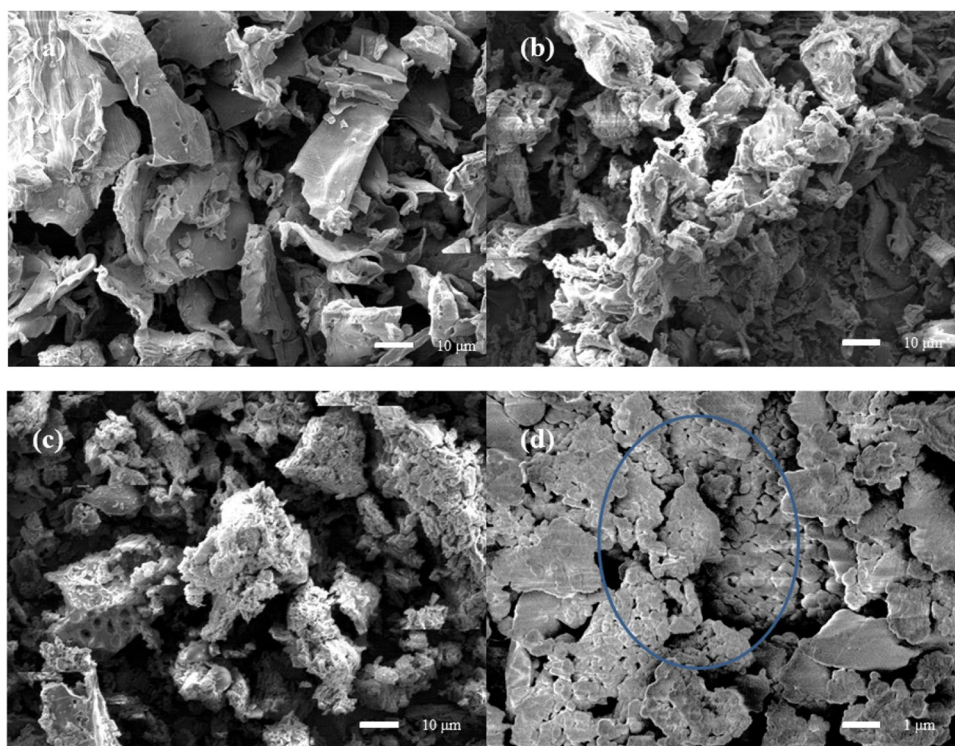


**Table 3** Total acid densities of the catalysts

Sample	Total acid densities (mmol $\text{g}^{-1}$ )
Catalyst-1	5.57
Catalyst-2	6.15
Catalyst-3	6.43

### 3.1.7 Acid densities analysis

The total acid densities of the catalysts were calculated according to the method of titration analysis from Eq. (1), and the analysis results were presented in Table 3.

It can be concluded that the acid densities ( $\text{SO}_3\text{H} + \text{COOH} + \text{OH}$ ) of Catalyst-3, Catalyst-2, and Catalyst-1 were 6.43, 6.15, and 5.57  $\text{mmol g}^{-1}$ , respectively. The acid densities of Catalyst-3 were highest among all samples. The results were consistent with the FTIR and elemental analysis. Also, the BET surface area of Catalyst-3 was much higher than Catalyst-1 and Catalyst-2. Although the total acid density of Catalyst-3 was the highest, the increase of specific surface area did not significantly increase the acid densities of solid acid. This proved that the  $-\text{SO}_3\text{H}$  groups of solid acid may be mainly concentrated on the surface of the catalysts.

## 3.2 Cellulose hydrolysis in LBTH

Analysis of TG, FTIR,  $\text{N}_2$  adsorption/desorption and elemental information revealed that the catalytic performance of Catalyst-3 was the best among the three catalysts. Therefore, the catalytic effect of Catalyst-3 was further evaluated by the reaction of cellulose hydrolysis in LiBr molten salt.

### 3.2.1 Influence of reaction time

In cellulose hydrolysis, the influence of reaction time was investigated at 110  $^\circ\text{C}$ . The histogram of results is presented in Fig. 9. It seemed that the conversion of cellulose to glucose readily generated in LBTH system, evidenced by rapid increase of glucose yield in the first 5 h. Upon longer reaction time, the glucose yield began to steady, and the highest yield of glucose was up to about 80%. However, during the hydrolysis reaction, the glucose dehydration is also detected, resulting in the by-product of levulinic acid, as shown in Fig. 9. It yet can be seen that the hydrolysis of glucose to levulinic acid was not severe, and the levulinic acid yield was only 4%. Even if there was a side reaction of glucose, a high-concentration sugar solution can still be obtained.

### 3.2.2 Influence of temperature

In most cases, raising the temperature could efficiently accelerate the rate of reaction. But in cellulose hydrolysis, a high temperature also boosted the conversion of glucose to

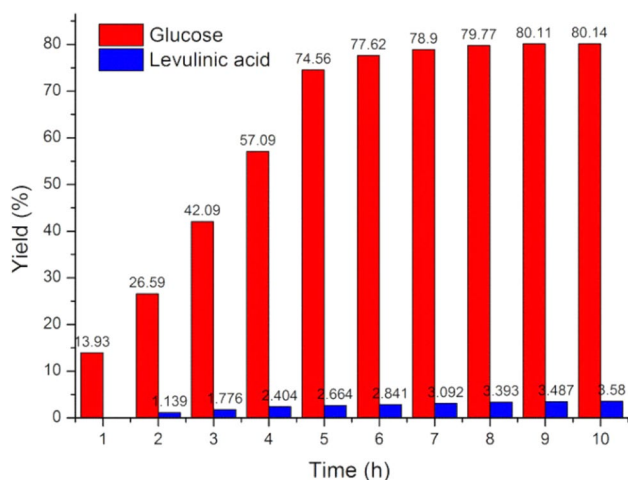


**Fig. 9** Hydrolysis yield at the temperature of 110 °C with Catalyst-3

degradation products. To obtain a high yield of glucose and avoid side reactions, a relatively low reaction temperature (90 °C–110 °C) was designed in this study. The effect of reaction temperature on cellulose hydrolysis catalyzed by Catalyst-3 is conducted, and the results are shown in Fig. 10. It was observed that glucose yield increased as temperature increased. When the reaction was carried out for 10 h, the yield of glucose was up to 80% at 110 °C, 73.8% at 100 °C, and 69.3% at 90 °C. This result suggested that cellulose could be easily hydrolyzed to glucose even at low temperature in the LBTH system. At the temperature of 90 °C, as the reaction progresses, the yield of glucose kept increasing at whole test period which indicates the reaction was not completed. At 100 °C, the reaction rate was accelerated, yet according to the curves, the reaction was still not able to reach a product yield plateau. While at 110 °C, a relatively

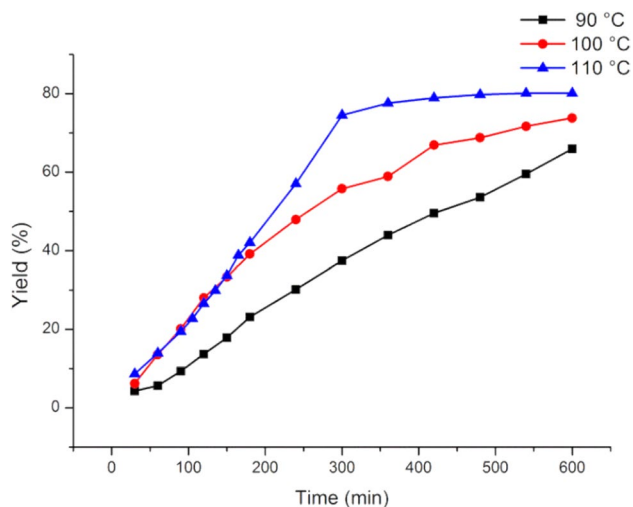


**Fig. 10** Effect of temperature on glucose yield

high yield can be obtained as early as at 300 min, and the glucose yield did not change much for a longer reaction time.

Levulinic acid, as the dehydration product of glucose, is also investigated, and the results are shown in Fig. 11. The yield trend of levulinic acid was somewhat similar to that of glucose. The yield increases with the elevated temperature. Fortunately, the dehydration of glucose to levulinic acid was not obvious at this system. Even at 110 °C, the yield of levulinic acid was only 3.58% after reaction for 600 min. Therefore, to obtain a high yield of glucose and inhibiting the formation of by-products, reaction at relatively low temperature with longer time was desired. However, low temperature will also reduce the reaction efficiency. Considering the tradeoff between efficiency and glucose yield, 110 °C was a suitable reaction temperature.

### 3.2.3 Comparison with other catalyst

Sulfuric acid was the most common homogeneous catalyst in cellulose hydrolysis. Therefore, we compared the catalytic effects of as-prepared catalyst with sulfuric acid. The catalytic effect of sulfuric acid catalyst is shown in Fig. 12.

By comparing Figs. 9 and 12, it can be found that the reaction rate of 0.02-M sulfuric acid is higher than that of the prepared solid acid. When the reaction proceeded for 2 h, the highest yield of glucose reached 71.01%, indicating that the homogeneous catalyst sufficiently contacted with cellulose in short time and effectively cut the  $\beta$ -(1–4) glycosidic linkages. However, although the reaction rate catalyzed by sulfuric acid was faster, the dehydration of glucose was also severe. After 10 h, the yield of levulinic acid had exceeded that of glucose. Serious dehydration of glucose was not conducive to obtaining high yield glucose.

It can be clearly seen from Fig. 13 that the reactant filtrate catalyzed by Catalyst-3 is colorless and clear, while

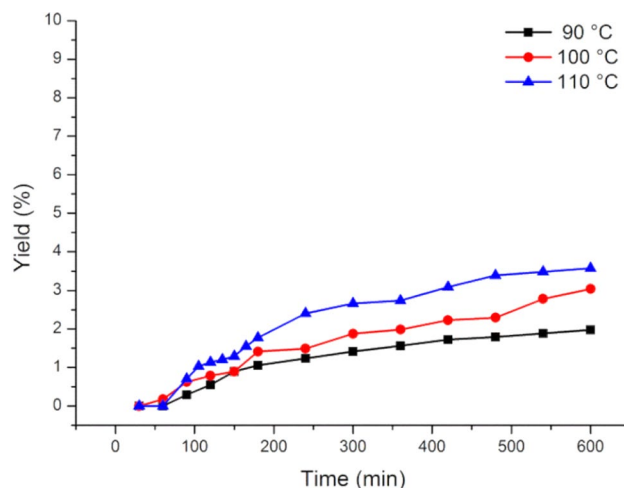


**Fig. 11** Effect of temperature on levulinic acid yield



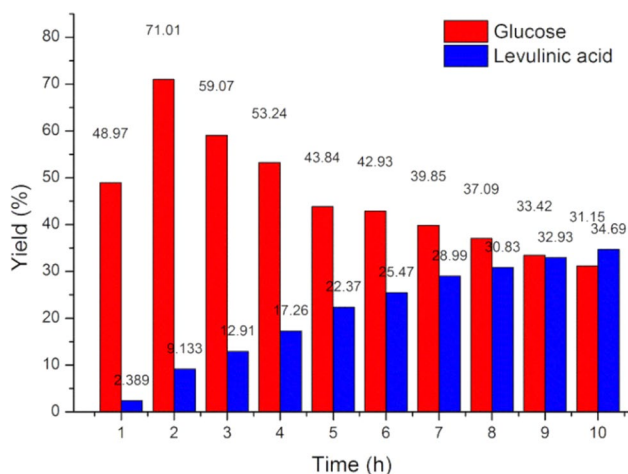


**Fig. 12** Hydrolysis yield at the temperature of 110 °C with sulfuric acid of 0.02 M

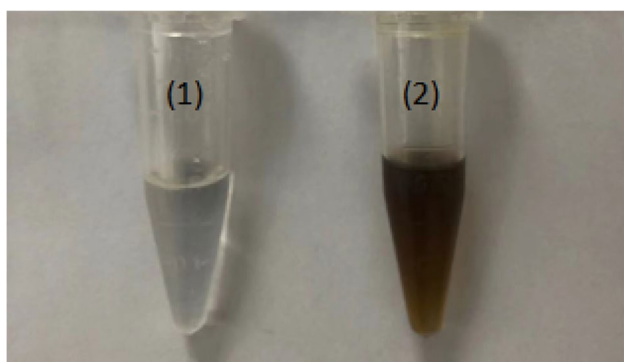


**Fig. 13** Reactant catalyzed by (1) Catalyst-3, (2) sulfuric acid for 10 h

the reactant catalyzed by sulfuric acid turns black brown. A darker color of sample indicated that a large amount of humins was formed in the process of reaction [44]. The presence of humins would pollute the solvent and make it difficult to separate glucose from the system. Overall, hydrolysis cellulose with the as-prepared Catalyst-3 in the LBTH system had the advantage of more mild, less glucose degradation, and no humins were produced.

The cellulose catalyzed by various solid acids in different solvent systems was further compared in Table 4. It was observed that the glucose yield was relatively low in water solvent. In comparison, in the LBTH or [BMIM]Cl/H<sub>2</sub>O polar system, the yield of glucose could be effectively increased. Particularly for cellulose hydrolysis, the yield of glucose catalyzed by Catalyst-3 in the LBTH system was relatively high compared with those reported from previous studies.

### 3.3 Insights of the cellulose hydrolysis in LBTH system catalyzed by solid acid

Cellulose was abundant with both intramolecular and intermolecular hydrogen bonds. The hydrogen bonds formed a certain steric hindrance, therefore –SO<sub>3</sub>H group of solid acid was difficult to attack the β-(1–4) glycosidic linkages in the aqueous system. However, in the LBTH system, cellulose could be fully dissolved, and the barrier of the hydrogen bond was easily broken. In the system, Li<sup>+</sup> has high charge density and oxygen affinity, and it was coordinated with H<sub>2</sub>O molecules. Br<sup>–</sup> was a much weakly bound anion, and it is almost free. The hydroxyl groups in cellulose combined with the incompletely hydrated lithium cations, leading to the disruption of hydrogen bond in cellulose [52]. Moreover, the hydroxyl group combined with Li<sup>+</sup> can effectively increase the hydrophilicity of cellulose and promote the dissolution of cellulose. The free Br<sup>–</sup> may interact with –OH in cellulose

**Table 4** Effect of cellulose hydrolysis with different solid acid catalyst

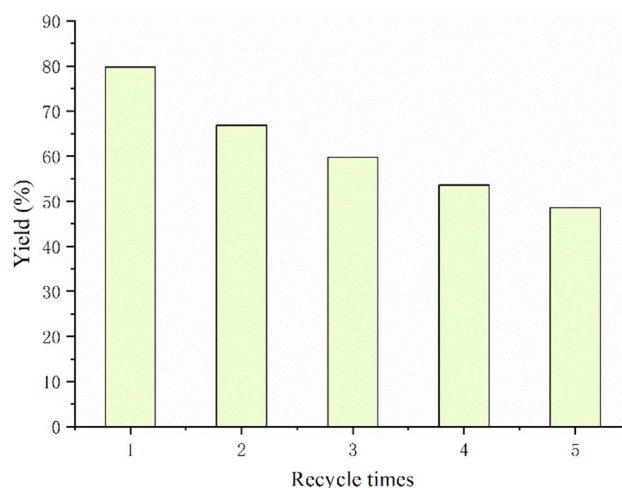
Serial number	Catalyst	Solvent	Temperature (°C) and time (min)	Glucose or TRS <sup>a</sup> yield (%)	Reference
1	Corncob-based solid acid	LBTH	110, 600	80.1	This work
2	H-zeolites	LBTH	140, 180	61.0	[10]
3	MLC–SO <sub>3</sub> H	[BMIM]Cl/H <sub>2</sub> O	140, 150	69.3	[15]
4	SC–SO <sub>3</sub> H	[BMIM]Cl/H <sub>2</sub> O	110, 240	63.0	[45]
5	HY zeolite	[BMIM]Cl/H <sub>2</sub> O	130, 120	50.0	[46]
6	[MIMPSH] <sub>n</sub> –H <sub>3–n</sub> PW	MIBK/H <sub>2</sub> O	140, 300	36	[47]
7	H <sub>3</sub> PW <sub>12</sub> O <sub>40</sub>	H <sub>2</sub> O	180, 120	50.5	[48]
8	Fe <sub>3</sub> O <sub>4</sub> –SBA–SO <sub>3</sub> H	H <sub>2</sub> O	150, 180	26.0	[49]
9	BC–SO <sub>3</sub>	H <sub>2</sub> O	90, 60	19.8	[50]
10	SCA–SO <sub>3</sub> H	H <sub>2</sub> O	130, 60	34.6	[51]

<sup>a</sup>TRS total reducing sugars

directly and facilitate the dissolution of cellulose. The catalytic mechanism of this process is proposed in Fig. 14; cellulose was dissolved in the LBTH system, and the hydrogen bonds of cellulose were interrupted. Then, the active sites of solid acids could contact and then cut the glycosidic bonds. Therefore, even under moderate conditions, the catalyst still had a high hydrolysis yield.

### 3.4 Recycling of catalyst

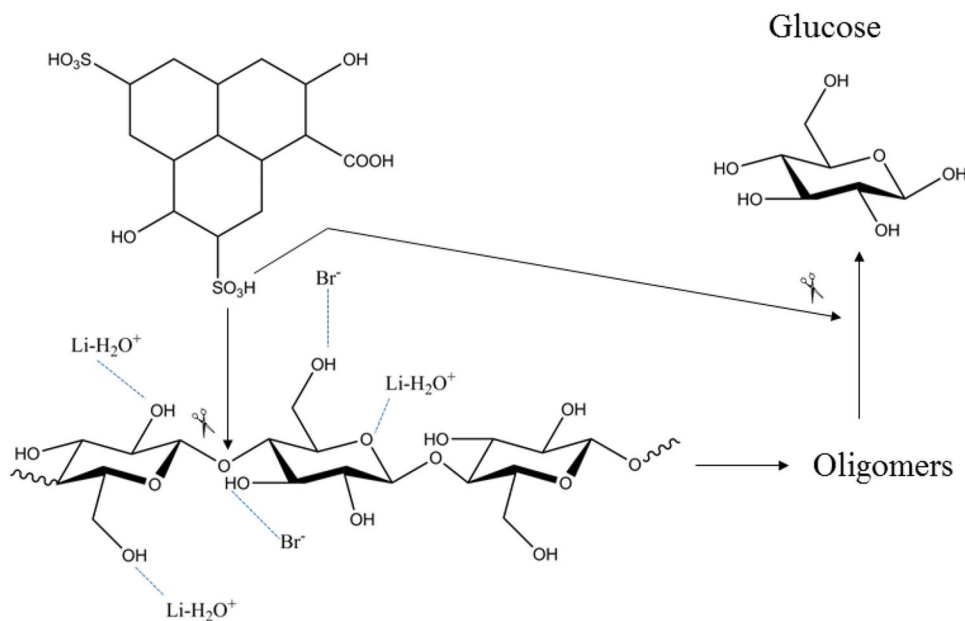
In addition to catalytic activity, the recyclability of a catalyst was an important indicator for catalyst performance. In commercial production, catalysts with excellent recyclability can significantly reduce costs. The recyclability of prepared catalyst was investigated, and the result is shown in Fig. 15. It was observed that the yield of glucose gradually decreased with the reuse of the catalyst. The glucose yield decreased from 80% (the 1st run), to 59.7% (3rd run), and 48.7% (5th run), respectively. The results showed that the catalyst was still active after several cycles. The total acid densities of the recycle process were also determined, and they are shown in Fig. 16. It can be seen from Fig. 16 that the total acid densities of solid acid decreases gradually in recycle, but catalyst activity decreased notably in the first reaction. The change of acid content was similar to that of the glucose yield. This phenomenon attribute to some colloidal carbon particles with  $-\text{SO}_3\text{H}$  sites being lost in the hydrolysis [53]. In polar reaction mixture as the LBTH system, the leaching of the carbon particles with  $-\text{SO}_3\text{H}$  groups from catalyst was more likely to appear [54]. In the first reaction, many unstable carbon particles with  $-\text{SO}_3\text{H}$  sites on the surface of solid acid were easily leached in LBTH system. As the number of recycle increases, the remaining active sites were relatively



**Fig. 15** Glucose yield in recycling process. (reaction conditions: 1-g cellulose, 0.5-g Catalyst-3, 45-g water, 55-g LBTH, 110 °C, 480 min)

stable, and the decrease in activity was not as remarkable as the first time. In addition, Catalyst-3 had high surface area with the microporous structures, therefore the soluble oligomers formed in the reaction may be adsorbed by these porous. The absorbed soluble oligomers may form a barrier between the acid active site and cellulose and then inhibit cellulose degradation to a certain extent [15]. This may be another factor for the decrease of glucose yield in the recycled catalyst.

**Fig. 14** Reaction mechanism of cellulose hydrolysis catalyzed by Catalyst-3 in LBTH system



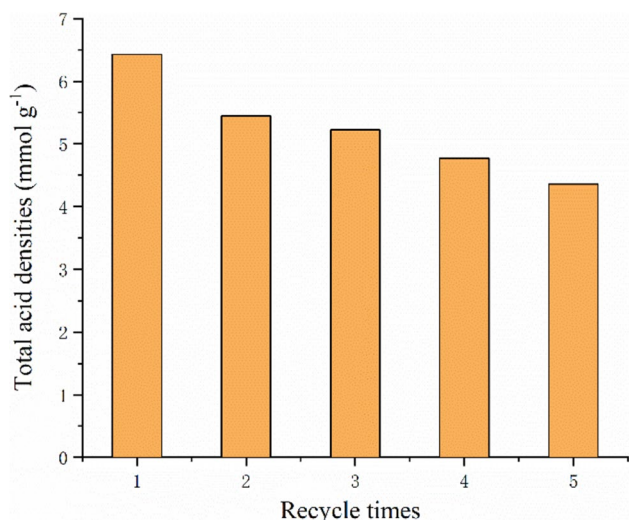


**Fig. 16** Total acid density of catalyst in recycling process (reaction conditions: 1-g cellulose, 0.5-g Catalyst-3, 45-g water, 55-g LBTH, 110 °C, 480 min)

## 4 Conclusion

In this work, three carbon-based solid acids (Catalyst-1, Catalyst-2, and Catalyst-3) derived from different corncob ingredients were prepared by the method of partial carbonization with sulfonation in succession. The Catalyst-3 presented the best catalytic activity with BET surface area of 338.23 m<sup>2</sup> g<sup>-1</sup> and total acid densities of 6.43 mmol g<sup>-1</sup>. The catalytic activity was tested through the hydrolysis of cellulose in the LBTH system and a high yield of glucose with 80.1% was achieved at a relatively moderate temperature of 110 °C for 6 h. Moreover, the catalyst remained effective after five successive runs. A plausible mechanism for the cellulose hydrolysis in LBTH system over the prepared solid acid was also proposed. The green utilization of corncob and high-efficiency hydrolysis of cellulose technology were elaborated in this work, which was of great significance for comprehensive utilization of corncob and cellulose conversion.

**Author contribution** All the authors contributed to this study. All the authors read and approved the final manuscript.

Chen Liang: writing—original draft preparation, funding acquisition, methodology

Chunhua Du: investigation

Xianli Wu: review and editing

Ju Wang: review and editing

Jie Xu: review and editing

Pengyu Hu: review and editing

Wangda Qu: investigation, writing—review and editing, funding acquisition

**Funding** This work was financially supported by the Doctoral Startup Foundation of Qingdao Agricultural University (No. 663/1120040),

Young Taishan Scholars Program of Shandong Province (No. tsqn 201909132), Natural Science Foundation of Shandong Province (No. ZR2020QB195), and Startup Foundation from Qingdao Agricultural University (No. 665/1119020).

**Data availability** Not applicable.

## Declarations

**Conflict of interest** The authors declare no competing interests.

## References

- Isikgor FH, Becer CR (2015) Lignocellulosic biomass: a sustainable platform for the production of bio-based chemicals and polymers. *Polym Chem* 6:4497–4559. <https://doi.org/10.1039/c5py00263j>
- Rackemann DW, Doherty WO (2011) The conversion of lignocellulosics to levulinic acid. *Biofuels Bioprod Bioref* 5:198–214. <https://doi.org/10.1002/bbb.267>
- Ma Z, Hu H, Sun Z, Fang W, Zhang J, Yang L, Zhang Y, Wang L (2017) Acidic zeolite L as a highly efficient catalyst for dehydration of fructose to 5-hydroxymethylfurfural in ionic liquid. *ChemSuschem* 10:1669–1674. <https://doi.org/10.1002/cssc.201700239>
- Jiang L, Zheng A, Meng J, Wang X, Zhao Z, Li H (2019) A comparative investigation of fast pyrolysis with enzymatic hydrolysis for fermentable sugars production from cellulose. *Bioresour Technol* 274:281–286. <https://doi.org/10.1016/j.biortech.2018.11.098>
- Sun S, Sun S, Cao X, Sun R (2016) The role of pretreatment in improving the enzymatic hydrolysis of lignocellulosic materials. *Bioresour Technol* 199:49–58. <https://doi.org/10.1016/j.biortech.2015.08.061>
- Qi W, Liu G, He C, Liu S, Lu S, Yue J, Wang Q, Wang Z, Yuan Z, Hu J (2019) An efficient magnetic carbon-based solid acid treatment for corncob saccharification with high selectivity for xylose and enhanced enzymatic digestibility. *Green Chem* 21:1292–1304. <https://doi.org/10.1039/c8gc02854k>
- Hammerer F, Loots L, Do J, Therien J, Nickels C, Friscic T, Auclair K (2018) Solvent-free enzyme activity: quick, high-yielding mechanoenzymatic hydrolysis of cellulose into glucose. *Angew Chem Int Ed* 57:2621–2624. <https://doi.org/10.1002/anie.201711643>
- Zhao X, Wang J, Chen C, Huang Y, Wang A, Zhang T (2014) Graphene oxide for cellulose hydrolysis: how it works as a highly active catalyst? *Chem Commun* 50:3439–3442. <https://doi.org/10.1039/c3cc49634a>
- Huang YB, Fu Y (2013) Hydrolysis of cellulose to glucose by solid acid catalysts. *Green Chem* 15:1095–1111. <https://doi.org/10.1039/c3gc40136g>
- Wu T, Li N, Pan X, Chen SL (2020) Homogenous hydrolysis of cellulose to glucose in an inorganic ionic liquid catalyzed by zeolites. *Cellulose* 27:9201–9215. <https://doi.org/10.1007/s10570-020-03411-3>
- Takagaki A, Tagusagawa C, Domen K (2008) Glucose production from saccharides using layered transition metal oxide and exfoliated nanosheets as a water-tolerant solid acid catalyst. *Chem Commun* 42:5363–5365. <https://doi.org/10.1039/b810346a>
- Yang H, Wang L, Jia L, Qiu C, Pang Q, Pan X (2014) Selective decomposition of cellulose into glucose and levulinic acid over Fe-resin catalyst in NaCl solution under hydrothermal conditions.

- Ind Eng Chem Res 53:6562–6568. <https://doi.org/10.1021/ie500318t>
13. Luo X, Wu H, Li C, Li Z, Li H, Zhang H, Li Y, Su Y, Song Y (2020) Heteropoly acid-based catalysts for hydrolytic depolymerization of cellulosic biomass. *Front Chem* 8:1–29. <https://doi.org/10.3389/fchem.2020.580146>
  14. Sahiba N, Agarwal DK, Manhas A, Sethiya A, Soni J, Jha PC, Agarwal S (2020) Mechanochemical approach for the selective synthesis of 1,2-disubstituted benzimidazoles and their molecular docking studies. *Polycycl Aromat Compd* 1–19. <https://doi.org/10.1080/10406638.2020.1768565>
  15. Hu L, Wu Z, Xu J, Zhou S, Tang G (2016) Efficient hydrolysis of cellulose over a magnetic lignin-derived solid acid catalyst in 1-butyl-3-methylimidazolium chloride. *Korean J Chem Eng* 33:1232–1238. <https://doi.org/10.1007/s11814-015-0267-8>
  16. Chen N, Zhang G, Zhang P, Tao X, Wu Y, Wang S, Nabi M (2019) Rice husk-based solid acid for efficient hydrolysis and saccharification of corncob. *Bioresour Technol* 292:121915. <https://doi.org/10.1016/j.biortech.2019.121915>
  17. Sahiba N, Sethiya A, Soni J, Agarwal S (2020) Metal free sulfonic acid functionalized carbon catalyst for green and mechanochemical synthesis of perimidines. *ChemistrySelect* 5:13076–13080. <https://doi.org/10.1002/slct.202003308>
  18. Sethiya A, Teli P, Manhas A, Agarwal D, Soni J, Sahiba N, Jha P, Agarwal S (2020) Carbon-SO<sub>3</sub>H: an efficient catalyst for the synthesis of biscoumarin under ambient reaction conditions and their in silico studies. *Synth Commun* 50:2440–2460. <https://doi.org/10.1080/00397911.2020.1780613>
  19. Hu L, Lin L, Wu Z, Zhou S, Liu S (2015) Chemocatalytic hydrolysis of cellulose into glucose over solid acid catalysts. *Appl Catal B Environ* 174–175:225–243. <https://doi.org/10.1016/j.apcatb.2015.03.003>
  20. Li M, Chen D, Zhu X (2013) Preparation of solid acid catalyst from rice husk char and its catalytic performance in esterification. *Chinese J Catal* 34:1674–1682. [https://doi.org/10.1016/s1872-2067\(12\)60634-2](https://doi.org/10.1016/s1872-2067(12)60634-2)
  21. Zhou Y, Niu S, Li J (2016) Activity of the carbon-based heterogeneous acid catalyst derived from bamboo in esterification of oleic acid with ethanol. *Energy Convers Manag* 114:188–196. <https://doi.org/10.1016/j.enconman.2016.02.027>
  22. Chin LH, Abdullah AZ, Hameed BH (2012) Sugar cane bagasse as solid catalyst for synthesis of methyl esters from palm fatty acid distillate. *Chem Eng J* 183:104–107. <https://doi.org/10.1016/j.cej.2011.12.028>
  23. Farabi MSA, Ibrahim ML, Rashid U, Taufiq-Yap YH (2019) Esterification of palm fatty acid distillate using sulfonated carbon-based catalyst derived from palm kernel shell and bamboo. *Energy Convers Manag* 181:562–570. <https://doi.org/10.1016/j.enconman.2018.12.033>
  24. Hussain Z, Kumar R (2018) Synthesis and characterization of novel corncob-based solid acid catalyst for biodiesel production. *Ind Eng Chem Res* 57:11645–11657. <https://doi.org/10.1021/acs.iecr.8b02464>
  25. Oh SJ, Jung SH, Kim JS (2013) Co-production of furfural and acetic acid from corncob using ZnCl<sub>2</sub> through fast pyrolysis in a fluidized bed reactor. *Bioresour Technol* 144:172–178. <https://doi.org/10.1016/j.biortech.2013.06.077>
  26. Liu W, Wu R, Wang B, Hu Y, Hou Q, Zhang P, Wu R (2020) Comparative study on different pretreatment on enzymatic hydrolysis of corncob residues. *Bioresour Technol* 295:122244. <https://doi.org/10.1016/j.biortech.2019.122244>
  27. Liang C, Hu Y, Wang Y, Wu L, Zhang W (2018) Production of levulinic acid from corn cob residue in a fed-batch acid hydrolysis process. *Process Biochem* 73:124–131. <https://doi.org/10.1016/j.procbio.2018.08.002>
  28. Zeng M, Pan X (2020) Insights into solid acid catalysts for efficient cellulose hydrolysis to glucose: progress, challenges, and future opportunities. *Catal Rev Sci Eng* 1–46. <https://doi.org/10.1080/01614940.2020.1819936>
  29. Weingarten R, Conner WC, Huber GW (2012) Production of levulinic acid from cellulose by hydrothermal decomposition combined with aqueous phase dehydration with a solid acid catalyst. *Energy Environ Sci* 5:7559–7574. <https://doi.org/10.1039/c2ee21593d>
  30. Yabushita M, Kobayashi H, Hara K, Fukuoka A (2014) Quantitative evaluation of ball-milling effects on the hydrolysis of cellulose catalysed by activated carbon. *Catal Sci Technol* 4:2312–2317. <https://doi.org/10.1039/c4cy00175c>
  31. Isik M, Sardon H, Mecerreyes D (2014) Ionic liquids and cellulose: dissolution, chemical modification and preparation of new cellulosic materials. *Int J Mol Sci* 15:11922–11940. <https://doi.org/10.3390/ijms150711922>
  32. Wang H, Gurau G, Rogers RD (2012) Ionic liquid processing of cellulose. *Chem Soc Rev* 41:1519–1537. <https://doi.org/10.1039/c2cs15311d>
  33. Bai Y, Xiao L, Sun R (2014) Efficient hydrolyzation of cellulose in ionic liquid by novel sulfonated biomass-based catalysts. *Cellulose* 21:2327–2336. <https://doi.org/10.1007/s10570-014-0287-2>
  34. Brennan TCR, Datta S, Blanch HW, Simmons BA, Holmes BM (2010) Recovery of sugars from ionic liquid biomass liquor by solvent extraction. *Bioenergy Res* 3:123–133. <https://doi.org/10.1007/s12155-010-9091-5>
  35. Thuy Pham TP, Cho CW, Yun YS (2010) Environmental fate and toxicity of ionic liquids: a review. *Water Res* 44:352–372. <https://doi.org/10.1016/j.watres.2009.09.030>
  36. Garkoti C, Shabir J, Mozumdar S (2017) An imidazolium based ionic liquid supported on Fe<sub>3</sub>O<sub>4</sub>@SiO<sub>2</sub> nanoparticles as an efficient heterogeneous catalyst for N-formylation of amines. *New J Chem* 41:9291–9298. <https://doi.org/10.1039/c6nj03985e>
  37. Yang X, Li N, Lin X, Pan X, Zhou Y (2016) Selective cleavage of the aryl ether bonds in lignin for depolymerization by acidic lithium bromide molten salt hydrate under mild conditions. *J Agric Food Chem* 64:8379–8387. <https://doi.org/10.1021/acs.jafc.6b03807>
  38. Li N, Li Y, Yoo CG, Yang X, Lin X, Ralph J, Pan X (2018) An uncondensed lignin depolymerized in the solid state and isolated from lignocellulosic biomass: a mechanistic study. *Green Chem* 20:4224–4235. <https://doi.org/10.1039/c8gc00953h>
  39. Deng W, Kennedy JR, Tsilomelekis G, Zheng W, Nikolakis V (2015) Cellulose hydrolysis in acidified ionic liquid molten salt hydrate media. *Ind Eng Chem Res* 54:5226–5236. <https://doi.org/10.1021/acs.iecr.5b00757>
  40. Liu Q, Ma Q, Sabnis S, Zheng W, Valchos DG, Fan W, Li W, Ma L (2019) Production of high-yield short-chain oligomers from cellulose: via selective hydrolysis in molten salt hydrates and separation. *Green Chem* 21:5030–5038. <https://doi.org/10.1039/c9gc02297j>
  41. Guo L, Hu Y, Wu L, Liang C, Zhang W (2018) The green hydrolysis technology of hemicellulose in corncob by the repeated use of hydrolysate. *Chinese J Chem Eng* 26:191–195. <https://doi.org/10.1016/j.cjche.2017.07.012>
  42. Liang C, Hu Y, Guo L, Wu L, Zhang W (2017) Kinetic study of acid hydrolysis of corncobs to levulinic acid. *BioResources* 12:4049–4061. <https://doi.org/10.15376/biores.12.2.4049-4061>
  43. Suganuma S, Nakajima K, Kitano M, Yamaguchi D (2008) Hydrolysis of cellulose by amorphous carbon bearing SO<sub>3</sub>H, COOH, and OH groups. *J Am Chem Soc* 130:12787–12793. <https://doi.org/10.1021/ja803983h>
  44. Zandvoort I, Wang Y, Rasrendra CB, Eck ERH, Bruijninx PCA, Heeres HJ, Weckhuysen BM (2013) Formation, molecular



- structure, and morphology of humins in biomass conversion: influence of feedstock and processing conditions. *Chemsuschem* 6:1745–1758. <https://doi.org/10.1002/cssc.201300332>
45. Guo H, Qi X, Li L, Smith RL (2012) Hydrolysis of cellulose over functionalized glucose-derived carbon catalyst in ionic liquid. *Bioresour Technol* 116:355–359. <https://doi.org/10.1016/j.biortech.2012.03.098>
46. Cai H, Li C, Wang A, Xu G, Zhang T (2012) Zeolite-promoted hydrolysis of cellulose in ionic liquid, insight into the mutual behavior of zeolite, cellulose and ionic liquid. *Appl Catal B Environ* 123–124:333–338. <https://doi.org/10.1016/j.apcatb.2012.04.041>
47. Sun Z, Cheng M, Li H, Shi T, Yuan M, Wang X, Jiang Z (2012) One-pot depolymerization of cellulose into glucose and levulinic acid by heteropolyacid ionic liquid catalysis. *RSC Adv* 2:9058–9065. <https://doi.org/10.1039/c2ra01328b>
48. Tian J, Wang J, Zhao S, Zhao S, Jiang C, Zhang X, Wang X (2010) Hydrolysis of cellulose by the heteropoly acid  $H_3PW_{12}O_{40}$ . *Cellulose* 17:587–594. <https://doi.org/10.1007/s10570-009-9391-0>
49. Lai D, Deng L, Guo Q, Fu Y (2011) Hydrolysis of biomass by magnetic solid acid. *Energy Environ Sci* 4:3552–3557. <https://doi.org/10.1039/c1ee01526e>
50. Wu Y, Fu Z, Yin D, Xu Q, Liu F, Lu C, Mao L (2010) Microwave-assisted hydrolysis of crystalline cellulose catalyzed by biomass char sulfonic acids. *Green Chem* 12:696–770. <https://doi.org/10.1039/b917807d>
51. Jiang Y, Li X, Wang X, Meng L, Wang H, Peng G, Wang X, Mu X (2012) Effective saccharification of lignocellulosic biomass over hydrolysis residue derived solid acid under microwave irradiation. *Green Chem* 14:2162–2167. <https://doi.org/10.1039/c2gc35306g>
52. Sen S, Martin JD, Argyropoulos DS (2013) Review of cellulose non-derivatizing solvent interactions with emphasis on activity in inorganic molten salt hydrates. *ACS Sustain Chem Eng* 1:858–870. <https://doi.org/10.1021/sc400085a>
53. Chen G, Wang X, Jiang Y, Mu X, Liu H (2019) Insights into deactivation mechanism of sulfonated carbonaceous solid acids probed by cellulose hydrolysis. *Catal Today* 319:25–30. <https://doi.org/10.1016/j.cattod.2018.03.069>
54. Mo X, López DE, Suwannakarn K, Liu Y, LoteroGoodwin EJG Jr, Lu C (2008) Activation and deactivation characteristics of sulfonated carbon catalysts. *J Catal* 254:332–338. <https://doi.org/10.1016/j.jcat.2008.01.011>

**Publisher's note** Springer Nature remains neutral with regard to jurisdictional claims in published maps and institutional affiliations.